COST EMF - MED (Action BM1309):
European network for innovative uses of EMFs in biomedical applications

STSM Report:

Examination of open-ended coaxial probe sensing volume for accurate dielectric measurements of complex biological tissues

Researcher: Alessandra La Gioia. Email: a.lagioia1@nuigalway.ie

Home Institution: Translational Medical Device Lab, National University of Ireland, Galway, Ireland. Contact: Martin O'Halloran. Email: martin.ohalloran@gmail.com

Host Institution: Keysight Technologies, Linz, Austria. Contact: Ferry Kienberger

STSM Reference: ECOST-STSM-BM1309-Examination of open-ended coaxial probe sensing volume for accurate dielectric measurements of complex biological tissues

STSM dates: FROM 27th February 2017 TO 17th March 2017

Abstract:

Accurate knowledge of the dielectric properties of biological tissue is fundamental for safety and dosimetry calculations, and electromagnetic medical diagnostic and therapeutic techniques. Dielectric properties of biological tissues are commonly measured using the open-ended coaxial probe. Although dielectric data acquisition with the open-ended coaxial probe appears quite straightforward, several factors can introduce uncertainties and errors into measured dielectric data. These errors can be related to the acquisition system or to the intrinsic properties of the investigated tissues. Generally, uncertainties are larger in dielectric measurements of heterogeneous tissues, due to their complex structure and composition. These confounders can be minimised by clearly defining the measurement sensing volume (defined by sensing radius and depth), and characterising the tissue distribution within that volume.

A. Purpose of the STSM

The Keysight slim form probe is the most applicable probe for measuring the dielectric properties of biological tissues [1]–[4]. The probe has been used in a number of tissue dielectric studies, including *in vivo* ones. Dielectric measurements with coaxial probes are based on the assumption that the measured material is homogeneous. Therefore, although the probe is regularly used with heterogeneous tissues, its function has not yet been well characterised in these heterogeneous scenarios.

For this reason, in this STSM, the Keysight slim form probe was used for dielectric measurements with the aim of:

- Evaluating the suitability of the ECal module for *in vivo* tissue dielectric measurements;
- Improving the protocol for the dielectric characterisation of heterogeneous samples.

Dielectric measurements are typically performed using an open-ended coaxial probe connected to one port of a vector network analyser (VNA) through a specialised cable. Specifically, ECal is a two port module that can be inserted between the cable and the probe. ECal can be used in dielectric measurement to automatically refresh the system calibration after the occurrence of a perturbation that introduces noise into

the dielectric data. The ECal suitability for *in vivo* measurements was tested by measuring the dielectric properties of aqueous electrolytic solution after perturbing the system. The system perturbation was introduced by moving and changing the cable position. The experiments were designed in order to simulate *in vivo* scenarios where the system is perturbed by bringing the probe into contact with the patient's body. With these experiments, it has been demonstrated that the use of the ECal module could be convenient for obtaining more accurate *in vivo* tissue dielectric measurements.

Furthermore, dielectric measurements of controlled heterogeneous samples were performed. Then, the acquired dielectric data was associated with the material percentage composition within the probe sensing volume. The experimental outcome was validated and integrated with the numerical results obtained by probe-material simulations. The integrated data provides information on how to interpret the dielectric properties of heterogeneous tissues, thus allowing refinement of the measurement protocol of tissue dielectric properties.

The details of these two sets of experiments are given in the section below.

B. Work Description

During the STSM two different types of experiments were carried out. In the first subsection, the experimental work to evaluate the suitability of the ECal module for *in vivo* measurements is explained. In the latter subsection, the heterogeneous samples and the simulations used to analyse the single material contribution to the total acquired dielectric data are described.

For both sets of experiments the dielectric measurement set-up shown in Figure 1 was used. The basic set-up consisted of:

- PNA-L N5230C, with frequency range of 10 MHz-50 GHz;
- Dielectric probes, with maximum frequency range of 200 MHz to 50 GHz (all the probes are composed of inner conductor, insulator, and outer conductor);
- Commercial software;
- Coaxial cable connecting the probe to the PNA;
- ECal module to refresh the calibration;
- Lift table to bring the sample towards the probe;
- Distilled (DI) water as load, one of the three mechanical standards besides short and air used in calibration (which details are reported in Figure 3);
- 0.1 M NaCl (prepared by mixing 5.844 g of salt in 1L of water) used to verify the quality of the calibration.

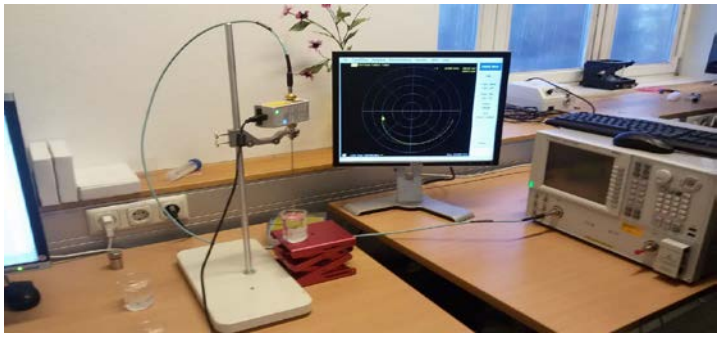

Figure 1: Experimental set-up for dielectric measurement

Evaluation of ECal performance and suitability for *in vivo* measurements

The performance of the ECal module was evaluated by comparing the 0.1 M sodium chloride solution measured before the dielectric system was perturbed by external movements and after the calibration refresh (following the perturbation) was automatically performed by ECal. The ECal performance was verified using all three types of probes (slim form, performance, and high temperature) included in the dielectric probe kit. The information about the three probes and the ECal module are schematised in Table 1. In this set of experiments, the 0.1 M sodium chloride solution was used since it has dielectric properties similar to those of biological tissues[5]–[7].

Keysight probe kit	Fabrication materials	Outer diameter	Frequency range	Sample size requirement
Slim form probe 	Outer conductor: Nickel Inner conductor: NA Insulator: NA	2.2 mm	500 MHz – 50 GHz	Minimum 5 mm insertion and 5 mm around tip of probe
Performance probe 	Outer conductor: Stainless steel Inner conductor: Nickel Insulator: Borosilicate glass	9.5 mm	500 MHz – 50 GHz	Minimum 5 mm insertion and 1 mm around tip of probe
High temperature probe 	Outer conductor: Inconel Inner conductor: Stainless steel Insulator: Borosilicate glass	19 mm	200 MHz – 20 GHz	Diameter > 20 mm
ECal module 	NA	Connector size compatible with all probes. The ECal module is connected, on one side, to the cable and, on the other side, to the probe.	300 KHz – 26.5 GHz	No restrictions

Table 1: Schematised characteristics of the Keysight dielectric probe kit.

The measurements with the performance and slim form probes were performed at 301 frequency points between 500 MHz - 20 GHz, and measurements with the high temperature probe were performed at 351 frequency points between 200 MHz – 20 GHz. For the high temperature probe measurements, more frequency points were used since the measurement frequency range was larger.

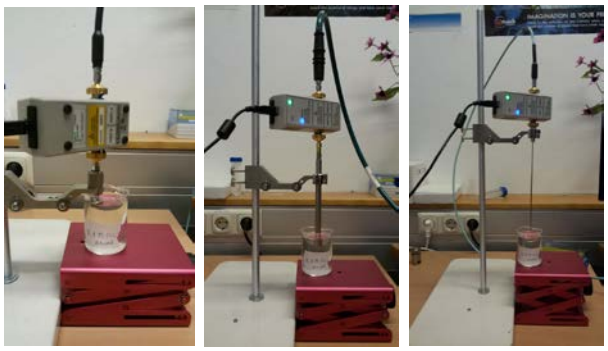

Figure 2: The three probes included in the Keysight dielectric probe kit and used in the experiments: from the left, high temperature probe, performance probe, and slim form probe.

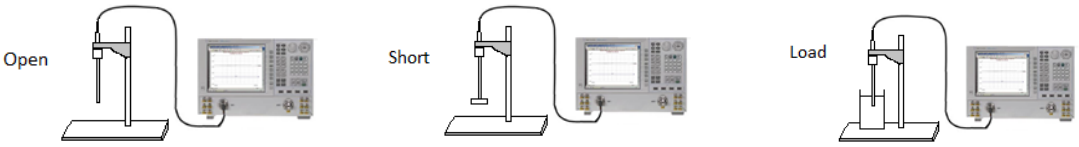

Figure 3: Illustration of the three standard calibration performed by the dielectric measurement of open, short, and load (DI water).

For the three probes, the standard protocol was followed using the commercial software. After checking the system connections, the three standard calibration was performed with ECal in line. The three standard calibration consists in the measurement of the dielectric properties of air, a metallic block (that short-circuits the probe tip), and a load with known dielectric properties, such as DI water. Specifically, the dielectric properties of the three standards were measured in order that the commercial probe software calculated and compensated for the three main systematic errors described in [8]. During the calibration procedure, the ECal module saved the three standard data that was used afterwards for the automatic refresh. The three standard calibration is illustrated in Figure 3. The quality of the calibration was verified by measuring the dielectric properties of the 0.1 M NaCl solution, one of the most commonly used reference liquids[5], [9]. The dielectric properties of the saline solution were measured using the commercial software after bringing the liquid sample to the probe tip. The measured dielectric signal was compared to the model described in [10]. In this way, the measurement accuracy, defined as the average percentage difference between the dielectric properties of the acquired data and the model, was calculated. If the measurement accuracy was within 3%, the calibration was determined to be of high quality and the measured 0.1 M NaCl signal was used as reference signal for the next measurements; otherwise the calibration procedure was repeated. After calculating the measurement accuracy, the system was perturbed. For the system perturbation, different cable positions and movement configurations were examined. The worst case scenario was chosen to test the ECal performance. In Figure 4, two examples of system perturbation are shown. The noise introduced into the dielectric system was quantified by re-measuring the 0.1 M NaCl solution after the perturbation. At this point, the performance of ECal was evaluated by comparing the 0.1 M NaCl solution measured after automatically refreshing the calibration with ECal to the saline reference signal.

The same procedure was performed with the slim form and performance probes without ECal in line and using the calibration refresh with air and water in order to provide a comparison and enable us to quantify the improvement in performance obtained by using the ECal.

A selection of the results obtained from the slim form probe are presented and discussed in Section C.

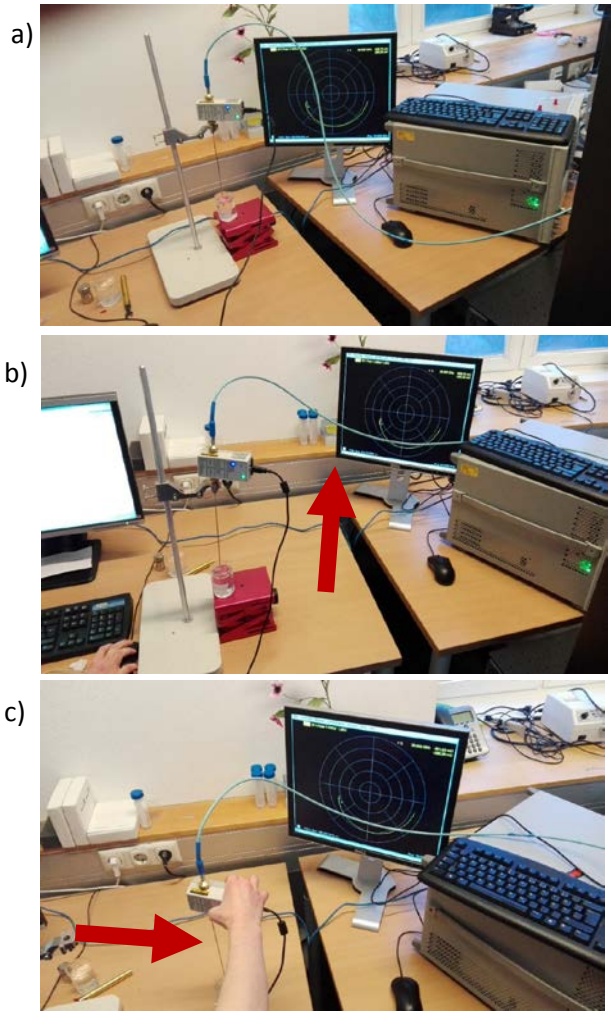

Figure 4: Two examples of system perturbation. a) Dielectric system after calibration; b) Dielectric system after cable movement and position change; c) Dielectric system after ECal position change without the use of the probe holder.

Impact of sample radial heterogeneities on the acquired dielectric data

The slim form probe was also used to evaluate how single materials contribute to the total permittivity signal of well-characterised and well-controlled heterogeneous samples. Firstly, radially heterogeneous samples were realised using PLA cylinders as sample inner material surrounded by DI water. Four cylinders having different radius and supported by a conical base were 3D-printed using polylactic acid (PLA). The four PLA 3D-printed objects, which are shown in Figure 5, have diameters of 1 mm, 1.2 mm, 1.5 mm and 2 mm, respectively. The cylinder size was chosen based on the 3D printer resolution and the probe sensing radius that is approximately equal to the probe diameter (2.2 mm), according to the findings in [11]. Further, DI water was chosen as sample outer material since it has high permittivity and represents a sharp contrast to the low permittivity of PLA (around 3).

Figure 5: PLA 3D-printed cylinders supported by a conical base and having radii of 0.5 mm, 0.6 mm, 0.75 mm and 1 mm, respectively.

Based on the slim form probe sensing radius, the percentage volume of PLA within the heterogeneous samples was calculated multiplying by 100 the ratio between the area of the cylinder circular section and the area of the probe tip (3.8 mm^2), while the percentage volume of DI water was calculated by subtracting the PLA percentage composition from the total percent composition of 100.

After characterising the radially heterogeneous samples, the material composition of each sample was associated to the correspondent dielectric data. The final radially heterogeneous samples are shown in Figure 6. The PLA cylinders were stuck to the bottom of a plastic box by double sided tape and then DI water was inserted. The experiments were conducted after performing and validating the three standard calibration (described in the previous subsection). Before taking the dielectric measurement, each sample was brought in contact with the probe tip by the lift table. The sample dielectric measurements were performed by positioning each PLA cylinder (immersed in DI water) in contact with the inner part of the probe tip. Uniform contact between the probe and the sample was ensured by performing close visual inspection. In this way, the samples were heterogeneous in the radial axis but unvarying in the longitudinal axis. Together with the heterogeneous sample measurement, also the permittivity and conductivity of DI water and PLA immersed in DI water were measured. The latest measurements were performed after placing a relatively large 3D printed PLA block on the bottom of a beaker before filling it with DI water. One measurement was performed in DI water in a beaker region far from the PLA block and the other measurement was performed on the PLA block. Since PLA is a rigid material, it was challenging to ensure a good probe-sample contact. Although the probe-PLA sample contact was monitored by visual inspection, the acquired permittivity was slightly higher than the actual one (the relative permittivity was around 5 instead of 3).

a)

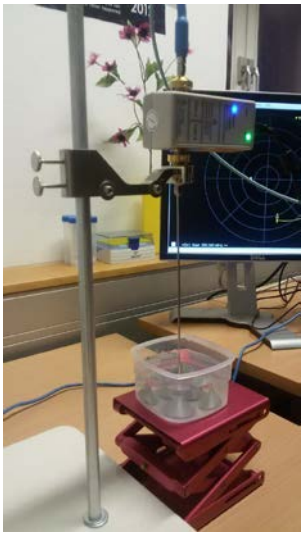

b)

Figure 6: a) Dielectric measurement of the 3D-printed cylinders immersed in DI water. b) Enlargement of the 1 mm radius cylinder in contact with the probe.

Lastly, the experimental results were validated by FEM simulations. The probe was modelled based on the data sheet specification [12]. The simulated S11 parameters of the probe in DI water were obtained using EMPro and COMSOL, then compared to the measured parameters. After verifying that the DI water simulation

S11 parameters closely matched the measured ones, all the experimental scenarios were simulated in COMSOL. COMSOL was preferred to EMPro, since it permits the use of a simplified 2D probe model which reduces the computational cost. The simulations helped verify the experimental outcome, since different confounders, such as probe-sample contact and pressure, could introduce errors in the dielectric measurements. The results are discussed in the following section.

C. Results

Evaluation of ECal performance and suitability for *in vivo* measurements

With the first set of experiments, it was demonstrated that the ECal module is convenient to use in situations where the system is perturbed and a calibration refresh is needed. The calibration refresh with Ecal is automatic and replaces the calibration refresh performed by mechanically placing one of the three standards (air, short, or DI water) in contact with the probe. In Figure 7, results obtained from the slim form probe are shown and the 0.1 M NaCl dielectric signals measured before the system perturbation (reference signal acquired after the standard calibration), after the system perturbation, and after the calibration refresh with ECal are compared. The signal acquired after the calibration refresh with ECal (in red in Figure 7) is totally comparable to the reference signal (in blue in Figure 7). In the permittivity and conductivity plots of Figure 7, the reference signal (in blue) is not clearly visible because it is overlapped to the signal acquired after the calibration refresh with ECal (in red). The good performance of the ECal module was furtherly confirmed by calculating the measurement accuracy, defined as the average percentage difference between the dielectric properties of the acquired data and the model in [10]. Precisely, the permittivity and conductivity data percent error values across the frequency range were obtained by the following formulas:

$$\epsilon\text{'error } [\%] = 100 \times \left| \frac{\epsilon\text{'measured} - \epsilon\text{'model}}{\epsilon\text{'model}} \right|$$

$$\sigma \text{ error } [\%] = 100 \times \left| \frac{\sigma \text{ measured} - \sigma \text{ model}}{\sigma \text{ model}} \right|$$

The permittivity and conductivity percent error values, ϵ'_{error} [%] and σ_{error} [%], were calculated for both the reference signal and the signal acquired after the calibration refresh with ECal (following the system perturbation). From the comparison of the acquired data to the saline model (Figure 7c), the data accuracy results to be within 1.3% even after the system perturbation and the calibration refresh with ECal.

a) b)

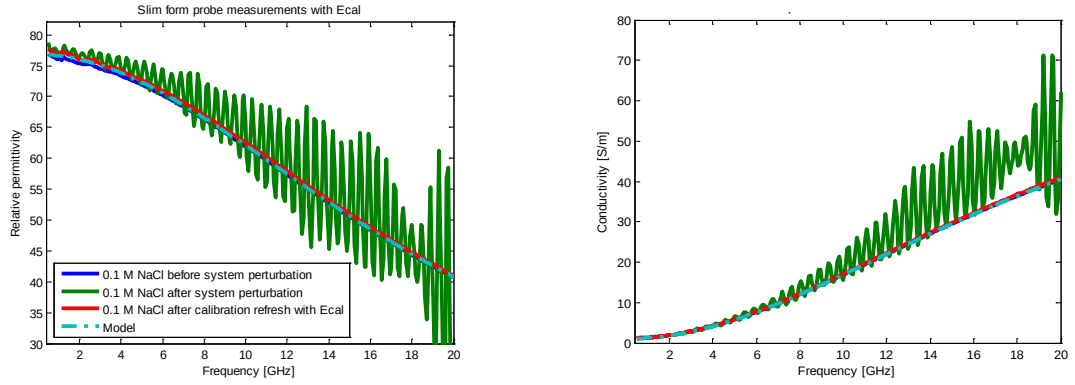

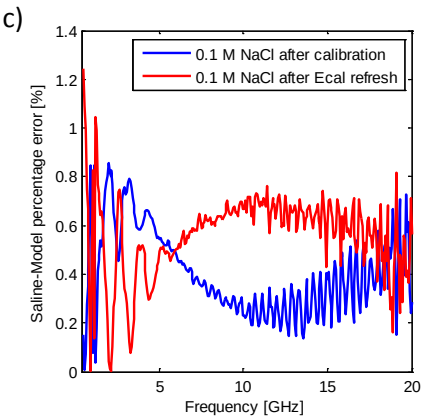

Figure 7: Comparison of the 0.1 M NaCl dielectric data acquired with the slim form probe after the system calibration, after the system perturbation, and after the calibration refresh with ECal in: a) relative permittivity and b) conductivity plots. The acquired data was also compared to the model in [10]. c) For both the measurements performed after the calibration and after the ECal calibration refresh following the system perturbation, the permittivity data accuracy is within 1.3%.

Equivalent results were obtained from the performance and the high temperature probe. Similar trends were also obtained without ECal in line and refreshing the calibration with DI water, although the calibration refresh with ECal has the advantage to be simpler, quicker and more suitable for tissue *in vivo* dielectric measurements.

Impact of sample radial heterogeneities on the acquired dielectric data

With the second set of experiments, the dielectric contribution of DI water and PLA within each radially heterogeneous sample was examined. In Figure 8, the dielectric data from the four samples is shown and compared to the dielectric traces of DI water and PLA immersed in DI water (the last measurement was performed on a PLA block larger than the probe sensing radius). Although, the material percentage composition of the four samples is very different, as reported in Table 2, the correspondent permittivity and conductivity signals have similar magnitude and are definitely more close to the PLA trace than the DI water one.

These early stage results suggest that the heterogeneous sample dielectric properties are not directly proportional to the percentage volume of each material within the sensing radius (and volume). Furthermore, it seems that the inner material has much higher impact on the total acquired dielectric signal.

PLA diameter (inner material)	**PLA percent area occupied in the 2.2 mm diameter sample**	**DI water percent area occupied in the 2.2 mm diameter sample**
2 mm	83%	17%
1.5 mm	46%	54%
1.2 mm	30%	70%
1 mm	21%	79%

Table 2: Material percentage composition of the four samples made of PLA (inner material) and DI water (outer material).

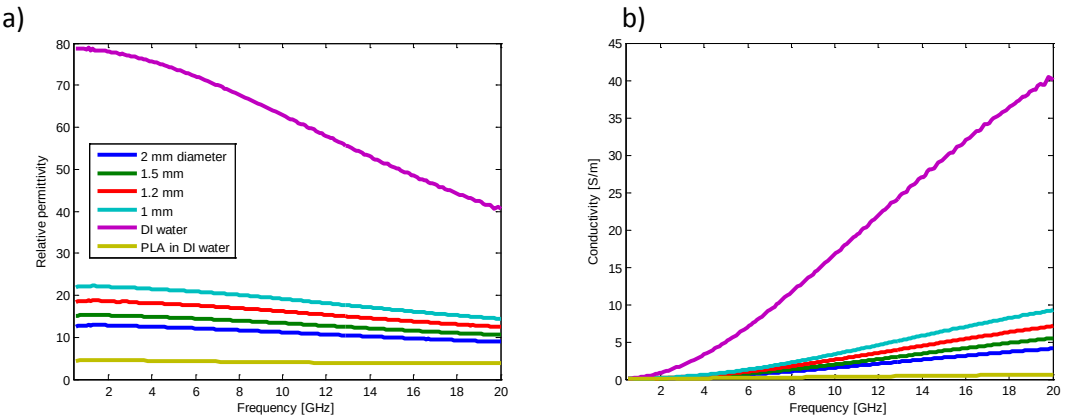

Figure 8: Comparison of the dielectric data from the four samples, DI water and PLA immersed in DI water in terms of: a) relative permittivity and b) conductivity.

In order to understand how the measured dielectric properties differ from those calculated taking into account the DI water and PLA percentage volumes within each sample, the percentage error between measured and estimated dielectric properties was calculated in the four scenarios. The correspondent plots are reported in Figure 9.

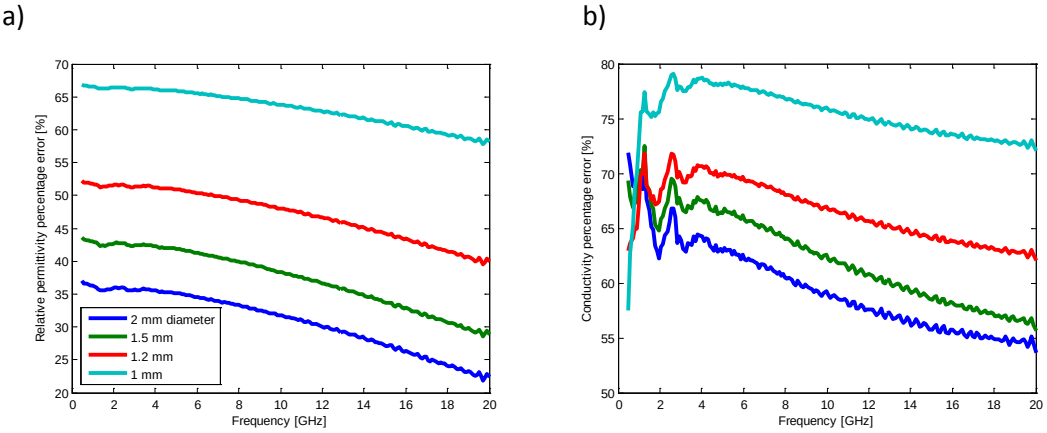

Figure 9: a) Relative permittivity and b) conductivity percentage error between measured dielectric properties and the dielectric properties estimated based on area occupied, from the four radially heterogeneous samples.

In both the permittivity and conductivity traces, the percentage error significantly increases as the PLA diameter decreases. This trend confirms that the inner material has a dominant dielectric impact on the acquired signal. This finding was qualitatively validated by simulating the heterogeneous scenarios in COMSOL.

As mentioned in the previous section, before simulating the heterogeneous scenarios, the probe model (based on the data sheet specification [12]) was used for simulations in DI water. The S11 parameters from DI water were compared to the measured ones. Specifically, the simulation was performed in a 2D environment taking advantage of the symmetry of the probe. In Figure 10, half longitudinal cross section of the probe tip in DI water is shown and the normal component of the electric field at 2 GHz is plotted. From the figure, it is possible to observe how the electric field propagates into the DI water from the inner conductor to the outer conductor. The electric field, after propagating along the coaxial probe (in TEM mode), fringes when it comes in contact with a material having different dielectric properties, such as DI water. The diagram suggests that the electric field magnitude is higher in correspondence of the inner probe conductor and the

probe sensing radius could be smaller than the probe radius. However, more investigation is needed to better quantify the probe sensing radius.

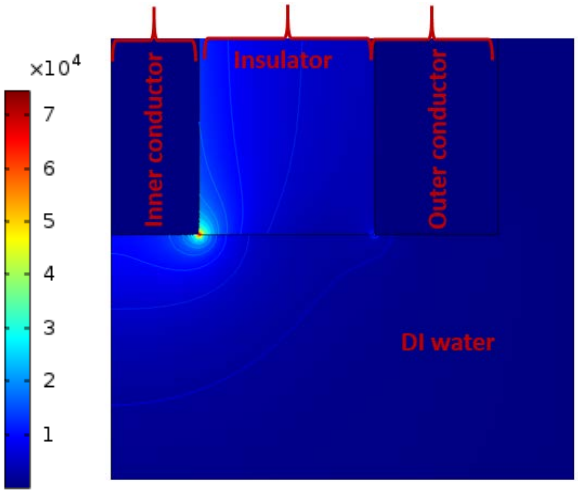

Figure 10: Enlargement the simulated slim form probe tip in DI water. In the simulation a simplified 2D axis-symmetric model was used and the electric field lines propagating from the inner conductor to the outer conductor through the DI water were plotted. Specifically, in this plot, the normal component of the electric field at 2 GHz obtained from simulating the probe in DI water is shown.

In Figure 11, the DI water S11 parameters from the simulation were compared to the measured one. The real part of the simulated and measured S11 parameters is well-matched, while a larger difference is found in the imaginary part of the S11 parameters at frequencies higher than 3 GHz. The difference in the imaginary part of the DI water S11 parameters may be due to differences between the modelled probe and the physical one, since the Keysight probe insulator and conductor materials are not detailed in the data sheet. Therefore, changes in the modelled probe material could result in a better match between simulation and measurement. However, considering the difference in probe material, there is a good match between the simulated and measured S11 parameters.

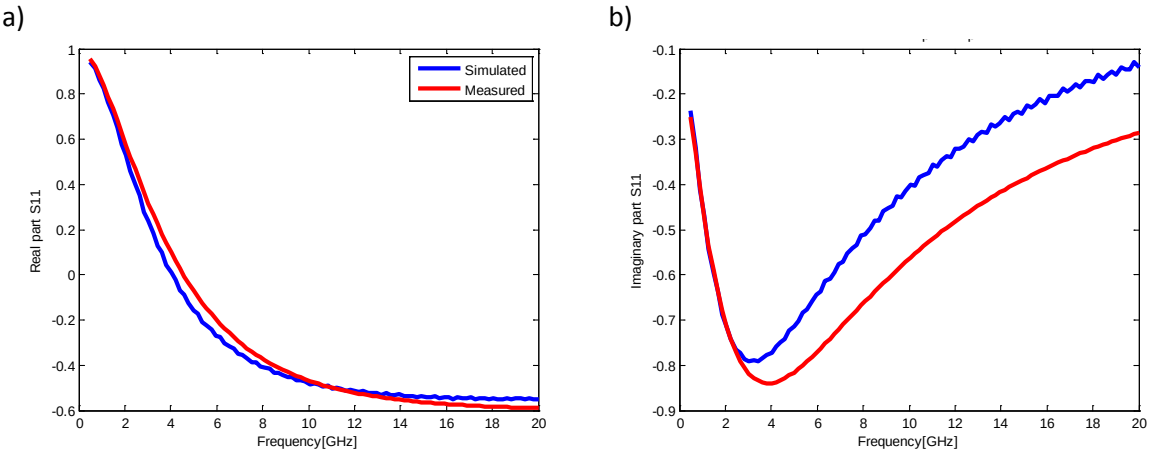

Figure 11: a) Real and b) imaginary part of DI water S11 parameters from both the simulation and the dielectric measurement.

The S11 parameters obtained from the simulations replicating each heterogeneous scenario were compared to the DI water and PLA simulation parameters. The traces of the real and imaginary part of the S11 parameters are reported in Figure 12. The trend of the S11 parameter traces is consistent with the permittivity and conductivity trend in Figure 7. As the PLA sample diameter gets smaller, the S11 parameters are closer to

the ones obtained from DI water, but still mostly similar to the S11 parameters of PLA. For instance, the S11 parameters from the 1 mm diameter PLA sample, composed of 21% PLA and 79% DI water, are very close to the S11 parameters from the 100% PLA block. Although the PLA composition of the heterogeneous sample is much lower than DI water, the reflection parameters are much closer to PLA than DI water. These simulation results confirm that the inner material has much more impact on the total signal acquired by the probe. In this way, the COMSOL simulations qualitatively validated the experimental outcome.

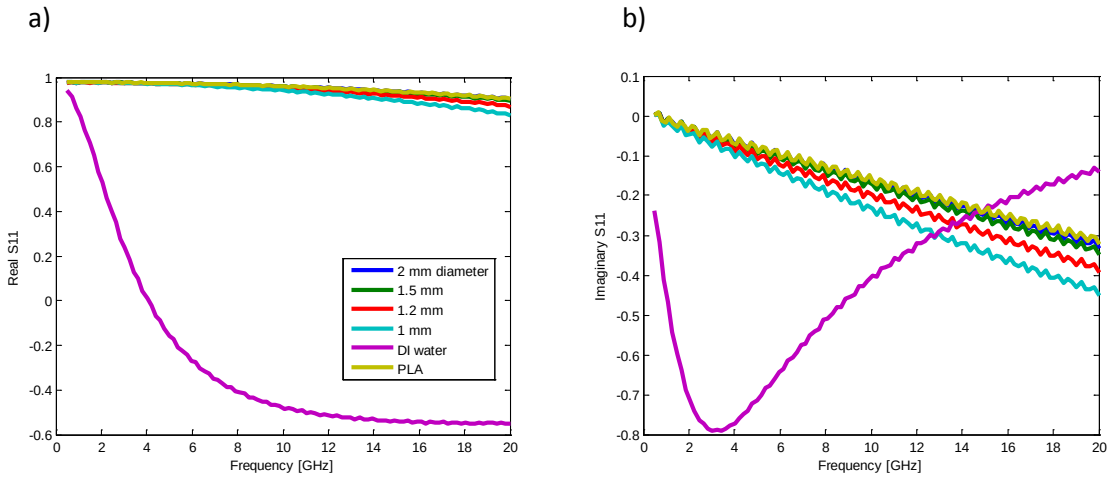

Figure 12: a) Real and b) imaginary part of S11 parameters obtained from the four heterogeneous scenarios and compared to the DI water and PLA simulation parameters.

In summary, both the simulation and the dielectric measurement outcome confirm that the signal acquired from the probe is not a weighted average of the materials present within the sensing radius, but the material closer to the probe inner conductor has more weight on the total data. These results provide the basis for a new interpretation of the dielectric properties collected from heterogeneous samples. Further experiments involving the analysis of different materials with specific complex structures across both radial and axial directions would improve the dielectric characterisation of heterogeneous biological tissues, thus allowing refinement of the measurement protocol of tissue dielectric properties.

To conclude, this work aims to provide the basis for more accurate dielectric properties to support EM medical device design and development.

D. Future collaboration with host institution

This STSM allowed the applicant to define the starting point for future collaborations with the host institution. Future works aim to refine the Keysight dielectric probe design and calibration procedure for more accurate dielectric measurements of biological tissues.

E. Expected Publications

It is planned to jointly publish work based in part on the outcome of this STSM.
Based on the knowledge obtained in this STSM and the planned work, we envisage to publish at least one joint conference work about the dielectric measurement of biological tissues using coaxial probes.

Confirmation by the host institution of the successful execution of the STSM:

We confirm that Alessandra La Gioia from National University of Ireland has performed the research work as described above. All the measurements were efficiently done with the best possible accuracy including calibration and systematic data capture.

Contact Person of Host Institution	Name of researcher
Ferry Kienberger	Alessandra La Gioia
Signature	Signature

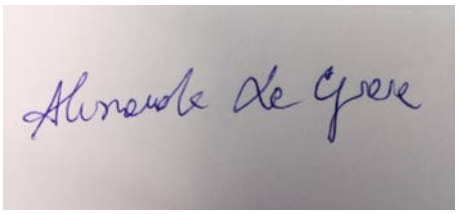

References

[1] T. Sugitani, S. Kubota, S. Kuroki, K. Sogo, K. Arihiro, M. Okada, T. Kadoya, M. Hide, M. Oda, and T. Kikkawa, "Complex permittivities of breast tumor tissues obtained from cancer surgeries," *Appl. Phys. Lett.*, vol. 104, no. 25, p. 253702, 2014.

[2] L. Abdilla, C. Sammut, and L. Mangion, "Dielectric properties of muscle and liver from 500 MHz-40 GHz," *Electromagn. Biol. Med.*, vol. 32, no. 2, pp. 244–252, 2013.

[3] R. J. Halter, T. Zhou, P. M. Meaney, A. Hartov, R. J. Barth, K. M. Rosenkranz, W. A. Wells, C. A. Kogel, A. Borsic, E. J. Rizzo, and K. D. Paulsen, "The correlation of in vivo and ex vivo tissue dielectric properties to validate electromagnetic breast imaging: initial clinical experience," *Physiol. Meas.*, vol. 30, no. 6, pp. S121–S136, 2009.

[4] A. Peyman, B. Kos, M. Djokić, B. Trotovšek, C. Limbaeck-Stokin, G. Serša, and D. Miklavčič, "Variation in dielectric properties due to pathological changes in human liver," *Bioelectromagnetics*, vol. 36, no. 8, pp. 603–612, 2015.

[5] A. Peyman, S. Holden, and C. Gabriel, "Dielectric Properties of Tissues at Microwave Frequencies," 2005.

[6] R. Buchner, G. T. Hefter, and M. P. May, "Dielectric relaxation of aqueous NaCl solutions," *J. Phys. Chem.*, vol. 103, no. 1, pp. 1–9, 1999.

[7] A. Stogryn, "Equations for Calculating the Dielectric Constant of Saline Water," *IEEE Trans. Microw.*

[8] H. Packard, "Automating the HP 8410B Microwave Network Analyzer," *Application Note 221A*. 1980.

[9] C. Gabriel and A. Peyman, "Dielectric measurement: error analysis and assessment of uncertainty," *Phys. Med. Biol.*, vol. 51, no. 23, pp. 6033–6046, 2006.

[10] A. Peyman, C. Gabriel, and E. H. Grant, "Complex permittivity of sodium chloride solutions at microwave frequencies," *Bioelectromagnetics*, vol. 28, no. 4, pp. 264–274, 2007.

[11] D. Hagl, D. Popovic, S. C. Hagness, J. H. Booske, and M. Okoniewski, "Sensing volume of open-ended coaxial probes for dielectric characterization of breast tissue at microwave frequencies," *IEEE Trans. Microw. Theory Tech.*, vol. 51, no. 4 I, pp. 1194–1206, 2003.

[12] Keysight, "N1501A Dielectric Probe Kit 10 MHz to 50 GHz: Technical Overview," 2015.